

1 **Performance of Composite Filters**
2 **Assembled from Multiple Layers of Basic Filtration Media**

3 **Peng Wang¹, Zhen Liu^{1,2} and Da-Ren Chen*¹**

4 *¹Particle Laboratory, Department of Mechanical and Nuclear Engineering,*
5 *Virginia Commonwealth University,*
6 *401 West Main Street, Richmond, VA, 23284*

7 *²Beijing Key Laboratory of Process Fluid Filtration and Separation,*
8 *College of Mechanical and Transportation Engineering,*
9 *China University of Petroleum, Beijing 102249, China*

10
11 **Abstract**

12
13 There is a severe shortage of face masks and N95 respirators due to the current COVID-19
14 pandemic, particularly in countries that were not well prepared in advance. In order to help ease
15 the supply demands of these resources, a strategy of using multiple layers of basic filtration media
16 to construct a composite filter that can match the particle collection efficiency offered by a N95
17 filtering facepiece respirator (FFR) is proposed. In this study, the filtration performances of four
18 face masks and one N95 respirator using the same test protocol (as a reference) were first compared.
19 Composite filter samples composed of multiple layers of basic face mask and MERV13 furnace
20 media were then constructed and the filter performance of the composite filters was investigated.
21 As expected, the minimum particle collection efficiency of the N95 respirator media sample was
22 higher than 95% and the efficiency of the samples from the four tested face masks varied from
23 71.8% to 83.6%. The Figure of Merit (FOM) values of the face mask samples were generally half
24 that of the N95 media sample. It was found that a N95-comparable collection efficiency can be
25 achieved by combining two/three layers of face mask media but at the expense of a higher media
26 pressure drop. Additionally, the composite filter samples made up of three/five layers of MERV13
27 furnace media could approach the FOM offered by the N95 media without the increased pressure
28 drop. It was also found that the measured collection efficiency of multiple-layered filter media was
29 not equal to the calculated in the test particle size range. Further studies are required to identify
30 the reason(s).

31
32 **Keywords:** COVID-19, N95 respirator, Face mask, Collection efficiency, Figure of merit

33
34

*Corresponding author: Da-Ren Chen, dchen3@vcu.edu

36 **1. Introduction**

37 COVID-19, the disease caused by Severe Acute Respiratory Syndrome CoronaVirus 2
38 (SARS-CoV-2), has been spreading globally since the first case reported in December 2019. This
39 new coronavirus has a higher mortality rate than the seasonal influenza and is more infectious than
40 either SARS or MERS (Middle East Respiratory Syndrome), the other known respiratory diseases
41 caused by coronaviruses (Liu et al., 2020; Prompetchara et al., 2020; Wilder-Smith et al., 2020).
42 Respiratory viruses can be transmitted via the droplets and droplet-nuclei produced by infected
43 individuals from coughing, sneezing, speaking, and even breathing (Yang et al., 2007; Stelzer-
44 Braid et al., 2009; Kutter et al., 2018). The World Health Organization (WHO) classifies
45 respiratory aerosols with diameters larger than 5 μm as droplets and those with diameters less than
46 5 μm as droplet-nuclei (WHO, 2014). Due to gravitational forces, large droplets settle quickly on
47 the mucosa of close contacts or environmental surfaces and can rarely travel more than 1-2 m from
48 their origination sources. For small aerosols, e.g., droplet nuclei, they can be suspended in the air
49 for a prolonged period of time and travel long distances from their sources (Xie et al., 2007;
50 Galton et al., 2011). Face masks have been used to prevent the transmission of respiratory aerosols
51 (MacIntyre et al., 2009; Cowling et al., 2010). Among the various face masks designed for
52 commonplace use, medical masks (also known as surgical/procedure masks) and filtering
53 facepiece respirators (FFRs) are the most commonly used. Medical masks are designed to protect
54 a sterile medical field from contamination by particles exhaled by patients and health workers, or
55 to reduce the exposure of healthcare workers to blood and other bodily fluids during medical
56 procedures. By their original design, medical masks are not appropriate for protecting wearers
57 from small respiratory particles due to their inadequate filtering and fitting attributes. In contrast,
58 FFRs are designed to cover the human nose and mouth tightly in order to protect wearers from

59 airborne particles, such as biological materials (e.g. mold, Bacillus anthracis, mycobacterium
60 tuberculosis), SARS viruses, Avian Flu, Ebola Virus, etc. and particulate matters (PM). FFRs thus
61 provide much better protection than face masks.

62 The US National Institute for Occupational Safety and Health (NIOSH) certifies FFRs
63 under regulation 42 CFR Part 84. Based on their resistance and media degradation, particulate
64 respirators are classified into the N (non-resistant), R (resistant), and P (proof) series. PPRs with
65 the minimum particle filtration efficiency of 95%, 99% and 99.97% are rated as 95, 99 and 100,
66 respectively. To measure the filtration efficiency, the FFRs in the N series are challenged by
67 continuously flowing neutralized polydisperse NaCl solid particles with a count median diameter
68 (CMD) of $0.075 \pm 0.020 \mu\text{m}$ and a geometry standard deviation (GSD) of >1.86 at a flow rate of
69 $85 \pm 4 \text{ L/min}$ through the respirators. Neutralized polydisperse dioctyl phthalate (DOP) liquid
70 particles with a CMD of $0.185 \pm 0.020 \mu\text{m}$ and a GSD of >1.6 are used for PPRs in the R and P
71 series. An entire FFR with the effective filtration area of 135 cm^2 is tested under the 85 L/min flow
72 rate, resulting in a face velocity of $\sim 10.5 \text{ cm/s}$. The mass concentration of particles upstream and
73 downstream of a test FFR are measured by a light-scattering photometer, under the condition that
74 the upstream particle concentration should not exceed 200 mg/m^3 . Table S1 lists the test standards
75 for the filtration efficiency of FFRs in various countries/regions for reference.

76 Surgical masks are cleared by the Food and Drug Administration (FDA) in the US. The
77 tested parameters for surgical masks include fluid resistance, particulate filtration efficiency (PFE),
78 bacteria filtration efficiency (BFE), differential pressure, and flammability. For the PFE, as shown
79 in Table S2, neutralized latex spheres in the size range of $0.1 \sim 5 \mu\text{m}$ and at a face velocity of $0.5 \sim$
80 25 cm/s are flowed through a circular sample of surgical mask media with a diameter of $50 \sim 150$
81 mm , according to the ASTM 2299 standard. Optical particle counters are used to measure the

82 particle number concentration both upstream and downstream of the filter sample under the
83 condition that the upstream particle number concentration should be less than 10^2 particles/cm³. In
84 contrast to the ASTM F2299 standard, un-neutralized polystyrene latex particles of 0.1 μ m in
85 diameter are recommended in the FDA guidelines. The BFE of surgical masks is tested using un-
86 neutralized staphylococcus aureus bacteria aerosols with a mean particle size (MPS) of 3.0 ± 0.3
87 μ m at a flow rate of 28.3 L/min against a whole surgical mask according to the ASTM F2101-19
88 standards and FDA guidelines. A six-stage viable particle cascade impactor is recommended for
89 collecting the bacterial aerosols. The bacterial aerosol delivery rate must be maintained at 1,700-
90 3,000 viable particles per test. The testing methods in other countries and regions are also given in
91 Table S2 for reference. No standard has been established in Europe or Japan for the PFE testing
92 of surgical masks. In comparison, FFRs and surgical masks are divided into various levels
93 according to their minimum filtration efficiency. Table S3 summarizes the efficiency level of face
94 masks in US, China, Europe and Japan. Note that it is known that the particle collection efficiency
95 of filter media depends on the size, shape, and charge status of particles; the electrical charge status
96 of the filter media; and face velocity. As shown in Tables S1 and S2, the testing of surgical masks
97 and FFRs was done under different conditions. Therefore, one cannot directly compare the
98 filtration efficiencies of surgical masks and FFRs simply based on the data obtained by the testing
99 standards presented.

100 The filtration performance of FFRs has been widely investigated (e.g., Brosseau et al., 1997;
101 Balazy et al., 2006a; Balazy et al., 2006b; Eninger et al., 2008; Rengasamy et al., 2008; Eshbaugh
102 et al., 2009; Rengasamy et al., 2009; Cho et al., 2010; He et al., 2013; Zuo et al., 2013). For
103 example, Balazy et al. (2006b) evaluated the filtration performance of N95 FFRs using NaCl
104 particles ranging from 10 to 600 nm in diameter. They found that the most penetrating particle

105 sizes (MPPS) of N95 FFRs were in the size range of 30-70 nm. The shift of the MPPS towards
106 nanometer-sized particles was found to be due primarily to the additional electrostatic collection
107 mechanism included in electret filter media which are commonly used in N95 FFRs. Eninger et al.
108 (2008) examined the performance of three FFRs, two N99 FFRs and one N95, with NaCl particles
109 in the sub-micrometer sizes and three virus aerosols, using flow rates of 30, 85, and 150 L/min.
110 They confirmed that the MPPS was less than 0.1 μm and that an increase in flow rate can
111 significantly increase the particle penetration. Rengasamy et al. (2008) tested five N95 and two
112 P100 FFRs with monodisperse silver particles of 4, 8, 12, 16, 20 and 30 nm at a flow rate of 85
113 L/min. They concluded the NIOSH-approved FFRs can provide the expected levels of filtration
114 efficiency against nanoparticles. Huang et al. (2013) examined the effects of face velocity, fiber
115 diameter, packing density, filter thickness, and fiber charge density on the filtration characteristics
116 of particulate respirators. They found that, for electret filter media, the MPPS increased with the
117 increase of fiber diameter and face velocity, and decreased with the increase of packing density,
118 thickness, fiber charge density, and filter thickness.

119 Others have investigated the performance of surgical masks (Willeke et al., 1996; Balazy
120 et al., 2006a; Lee et al., 2008; Oberg and Brosseau, 2008). Willeke et al. (1996) measured the
121 penetration of bacteria with different shapes and aerodynamic sizes through surgical masks under
122 various flow rates and compared them with the penetration of oil particles of the same aerodynamic
123 sizes. It was found that the penetration of surgical masks decreased with an increased aspect ratio
124 of the bacterial dimensions, and that the penetration of spherical particles is always higher than
125 that of bacteria particles. Balazy et al. (2006a) measured the filtration efficiency of two surgical
126 masks with the MS2 virus in the particle size range of 10-80 nm under the inhalation flow rate of
127 85 L/min. They observed that some surgical masks may provide very low protection against

128 airborne viruses in this size range. Lee et al. (2008) did human test subject evaluations for four
129 FFRs and three surgical masks using NaCl particles in the 0.04-1.3 μm size range. They showed
130 that the protection factor (i.e., the ratio of particle concentration outside the respirator to that of
131 inside the respirator, which is equal to the reciprocal of the particle penetration) of surgical masks
132 was 8-12 times less than that of FFRs on average. Oberg and Brosseau (2008) measured the
133 penetration of 9 surgical masks using monodisperse latex spheres of 0.895, 2.0 and 3.1 μm
134 diameters at the flow rate 6 L/min and polydisperse NaCl particles with a CMD of 0.075 μm at the
135 flow rate of 84 L/min. They concluded that surgical masks exhibited a wide range of 0%-84%
136 particle penetrations for latex particles of three selected sizes and a similar range of 4%-90% for
137 the penetration of NaCl particles.

138 Though the filtration performance for large bacteria has been reported, limited research has
139 been done on the filtration of surgical masks for ultrafine particles in the virus size range. Due to
140 difference testing standards, it is difficult to make direct comparisons on the filtration performance
141 (i.e. particle collection efficiency) of FFRs and surgical masks. Moreover, the wide-spread urgent
142 demand of N95 FFRs during the current COVID-19 pandemic has resulted in a severe shortage of
143 N95 FFRs in various countries/regions, especially in the ones ill-supplied before the pandemic.
144 The strategy of using multiple layers of basic filter media such as those used in face masks and
145 furnace filter media to construct composite filter media with particle collection efficiencies
146 matching that offered by N95 FFRs is proposed as an alternative to N95 FFR media. The pros and
147 cons of this strategy have not been scientifically investigated to the authors' knowledge (although
148 the general rule of thumb is known). The objectives of this study are thus to (1) directly compare
149 the filtration performance of FFRs and surgical masks under the same testing protocol using NaCl
150 particles to represent virus particles (Eninger et al., 2008; Davidson et al., 2013); (2) study the

151 filtration performance of composite filters, assembled by loosely layering multiple layers of basic
152 filtration media that are readily available in the market; and (3) examine the additivity of the
153 filtration performance of the above composite filters.

154 **2. Experimental protocol**

155 **2.1 Experimental setup**

156 Figure 1 shows a schematic diagram of the experimental setup used in this study. A custom-
157 made Collison atomizer with NaCl solution (2% NaCl by volume in DI water) was used to generate
158 polydisperse NaCl droplets. The produced NaCl droplets were passed through the diffusion dryer
159 with silica gel as the desiccant to obtain solid NaCl particles. A bypass line with a HEPA filter and
160 a needle valve as the aerosol flow exhaust line was included in the setup in order to vary the flow
161 rate of the aerosol stream entering the Differential Mobility Analyzer (DMA, TSI 3081). Before
162 the aerosol stream enters the DMA, it is directed through a Kr⁸⁵ neutralizer which is included in
163 the DMA platform TSI 3080 to achieve a stationary charge distribution on the NaCl particles. The
164 DMA was operated at aerosol and sheath flow rates of 0.5 and 3 L/min, respectively, for the
165 classification of particles based on their electrical mobilities. By fixing the DC voltage on the
166 DMA, particles having the electrical mobilities in a narrow range were classified and passed
167 through a Po²¹⁰ neutralizer to reduce the particle charge status to the stationary state. The DMA-
168 classified particles were then used as test particles. By varying the DMA voltage, particles with
169 different electrical mobilities could be selected. During the filter testing, the upstream
170 concentration of particles was kept as low as possible ($\sim 10^3$ #/cm³) to prevent the test filter sample
171 from the particle loading. It is the basis for testing the filter samples using particles in a narrow
172 size distribution instead of ones in a wide size distribution.

173 A test filter sample was placed in a 47mm inline filter holder with an effective filtration
174 area of 10.15 cm². A make-up air line with a HEPA filter capsule was included before the filter
175 holder to passively introduce clean air from the ambient environment into the setup. The total flow
176 rate through the filter holder was set at 6.4 L/min, which is equivalent to a flow rate of 85 L/min
177 for a whole FFR with a filtration area of ~135 cm² providing a face velocity of ~10.5 cm/s. An
178 Ultrafine Condensation Particle Counter (UCPC, TSI 3776) and a Condensation Particle Counter
179 (CPC, TSI 3775), operated at the 1.5 L/min high flow mode, were used to measure the particle
180 concentrations upstream and downstream of the filter holder, respectively. A HEPA filter capsule
181 was installed downstream of the filter holder to collect particles penetrating through the test filter
182 sample. A mass flow meter (TSI 4000), a needle valve, and a vacuum pump were installed after
183 the HEPA capsule to pull the 4.9 L/min air flow through the line. The required test flow rate of 6.4
184 L/min was obtained by adding the CPC sampling flow rate (1.5 L/min) and the 4.9 L/min air flow
185 rate. A differential pressure transducer (OMEGA PX655-01DL) was used to measure the pressure
186 drop across the test filter sample. Prior to the efficiency measurement, an experiment to calibrate
187 both CPC readings by feeding DMA-classified particles into the two CPCs (with no filter sample
188 in the filter holder) was conducted. The background pressure drop across the empty filter holder
189 was also measured for data analysis.

190 **2.2 Test filter samples and data analysis**

191 Filter samples punched out from one N95 FFRs and four face masks (one surgical mask,
192 one procedure mask, one face mask with coconut shell activated carbon, and one single-use
193 medical mask) were tested in this part of the study. In addition, furnace filter media with the
194 minimum reported efficiency value of 13 (MERV 13) was also included as one of the basic
195 filtration media in the alternative FFR filter media part of this study. Table 1 shows the label

196 designation and rated particle filtration efficiency of the test filter media provided by the
197 manufacturers. Composite filter media assembled from multiple layers of mask/furnace filter
198 media listed in Table 1 were also tested. The measured pressure drops across all the test filter
199 samples at the face velocity of 10.5 cm/sec are given in Table 2.

200 For the particle collection efficiency measurements in this study, test particles with the
201 DMA-classified diameters of 20, 30, 50, 75, 100, 150, 200, 300, 400, 600, and 800 nm were used.
202 The collection efficiency of each filter sample at a given particle size was calculated as:

$$E = \left(1 - \frac{C_{down}}{C_{up}}\right) \times 100\% \quad (1)$$

203 where E is the particle collection efficiency of a test filter sample and C_{down} and C_{up} is the average
204 particle number concentrations downstream and upstream of a test filter sample, respectively. The
205 collection efficiency based on particle number concentration was selected for use in this study
206 because this testing method is more rigorous than that of the method based on mass concentration
207 for evaluating the worst-scenario performance of a filter sample (Rengasamy et al., 2011). At least
208 three filter samples randomly selected from each face mask and FFR were tested in each case and
209 the averages of the measured data were reported. The pressure drop of each filter sample was also
210 measured at the beginning and ending of the filtration testing to ensure no particle loading effect
211 occurred during the testing.

212 The Figure of Merit (FOM) for a filter sample of a specific size can be calculated as:

$$f = \frac{-\ln(1 - E)}{\Delta P} \quad (2)$$

213 Where f is the figure of merit (units of Pa⁻¹) and ΔP is the pressure drop in units of Pa. Note that
214 the FOM is not dimensionless and depends on the unit selected for the pressure drop.

215 **3. Results and discussion**

216 **3.1 Comparison of filtration efficiency of respirator and mask filter samples**

217 Figure 2 shows the size-fractionated filtration efficiency of filter samples obtained from
218 the FFR and the four face masks as the function of the particle size under a face velocity of 10.5
219 cm/sec. For all the test sizes, the collection efficiency of the electret N95 FFR sample was much
220 higher than that of the face mask samples. Its minimum particle efficiency was more than 95% at
221 the most penetration particle size (MPPS) of ~50 nm. For a FFR sample with electret media, the
222 particle diffusion dominates in the media for collecting particles of sizes less than 50 nm, while
223 both interception and electrostatic mechanisms play major roles in the media to remove particles
224 of sizes larger than 50 nm (Romay et al., 1998). The MMPS was found to be the particle size in
225 which the transition from diffusion-dominated collection to interception and electrostatic force-
226 dominated collection occurs. The particle collection efficiency of the face mask samples at the
227 MMPS varied from 71.8%-83.6%. Filter sample B, taken from a surgical mask, having the lowest
228 particle collection was expected due to its usual application in dental service. The MPPS of all the
229 face mask samples was measured to be ~50nm, which is close to that of the electret FFR filter
230 sample. This observation implies that all the face masks selected in this study were likely made of
231 different grades of electret filter media. Figure. 3 shows the FOM for each filter sample as a
232 function of the particle size. The N95 FFR sample has a higher FOM value compared to all the
233 face mask samples, particularly for large particles. Except for the low FOM of the filter sample D,
234 the filter samples from the other three face masks had very close FOM curves (as a function of the
235 particle size).

236 **3.2 Composite media matching the collection efficiency of N95 FFRs**

237 One simple way of constructing alternative media for N95 FFRs is by combining multiple
238 layers of basic filtration media. Face masks and furnace filter panels are readily available on the
239 market and were thus selected as basic filtration media in this part of the study. Figure 4 shows the
240 particle collection efficiency of the multi-layered composite filter samples at the selected particle
241 sizes under the face velocity of 10.5 cm/sec. It is shown that for all the test sizes, the particle
242 collection efficiencies of double- and triple- layered mask filter samples are significantly higher
243 than that of their basic filtration media counterparts (shown in Fig. 2). Triple-layered B media and
244 double-layered C, D, E media samples have collection efficiencies of more than 93% for particles
245 larger than 100 nm. Figure 4 also shows that the MMPS remained unchanged by doubling/tripling
246 the face mask media. Since the typical particle size range of SARS-CoV-2 is between 60 to 140
247 nm, with a mean diameter of 100 nm measured by electron micrographs (Zhu et al., 2020),
248 double/triple-layered face masks can offer comparable protection from SARS-CoV-2 to that of a
249 N95 respirator from the viewpoint of particle collection efficiency.

250 The particle collection efficiency of three- and five-layer MER 13 furnace filter media (i.e.,
251 Media F) test samples as a function of the particle size is also included in Figure 4. Furnace filter
252 media was selected as another basic filtration media because it is widely available in the hardware
253 stores during the COVID-19 pandemic and low in cost. More importantly, it is electret filter media
254 of low grades. As shown in Figure 4, composite filter samples with triple layers of the selected
255 furnace filter media have collection efficiencies higher than 95% for particles larger than 100 nm.
256 The filter samples' efficiencies were, however, less than 95% for particles smaller than 100 nm,
257 because of the wide opening in low grade electret media compared to that of N95 FFR media. For
258 particles larger than 100 nm, electrostatic forces dominate in particle collection within electret
259 media, resulting in a high particle collection efficiency. For particles less than 100 nm in diameter,

260 the particle collection of the media by electrostatic forces is weakened due to the small particle
261 sizes. Collection by particle diffusion in the furnace filter media is also not very effective due to
262 the wide-open microstructure of the media compared to the N95 FFR media. For the sample with
263 five layers of basic furnace filter media, its collection efficiency increased significantly for
264 particles in the sizes less than 100 nm because of the increased particle residence time in the sample.
265 As a result, the minimum particle collection efficiency of five-layered furnace media composite
266 sample was 94.6% compared to 84.9% for the three-layers media sample. Notice that the MPPS
267 of the five-layered furnace media composite sample was at ~30 nm, smaller than that of the N95
268 respirator and the face masks.

269 The trade-off in using composite filters constructed from multiple layers of basic filtration
270 media to achieve the N95 FFR media efficiency is typically assumed to be the increased filter
271 pressure drop (compared to the N95 FFRs). The pressure drops for a given multi-layered composite
272 filter sample was assumed to be the sum of the pressure drops of the individual media layers.
273 Figure 5 shows the FOM of the multi-layered mask and furnace media composite samples as a
274 function of the particle size. The FOM of the N95 FFR sample is also included in Figure 5 as a
275 reference. A negligible difference in the FOM curves was observed among all the multi-layered
276 face mask samples. Additionally, the FOM values of face mask composite samples were generally
277 lower than that of the N95 FFR sample (~ half the FOM value of the N95 FFR sample). This data
278 proves that the N95-comparable efficiency of double/triple- layered mask composite samples is
279 indeed achieved at the expense of an increased pressure drop for most cases using face mask
280 samples. However, in the cases of the composite filter samples made of multiple layers of furnace
281 filter media, their FOM values were higher than that of the N95 FFR sample, particularly for
282 particles larger than 100 nm. Based on the FOM values given above, composite filters made of

283 multiple furnace filter media layers would be preferred as an alternative for a N95 FFR. Notice
284 that although the FOM values for the composite samples made of multiple layers of face mask
285 filter media were less than that of the N95 FFR sample, the pressure drops for all the tested
286 composite samples remained within the allowable pressure drop range (i.e. < 350 Pa) for a N95
287 FFR.

288 **3.3 On the additivity of composite filters made of multiple layers of basic filtration media**

289 It is typically assumed that the penetration of composite filters, which is made of multiple
290 layers of basic filtration media, is equivalent to the product of the penetration efficiency of the
291 individual filtration media layers functioning independently. The particle collection efficiency of
292 the composite filter samples can be calculated by Eq. (3):

$$\eta_n = 1 - (1 - \eta_s)^n \quad (3)$$

293 where n is the number of basic media layers in a composite filter and η_s is the collection efficiency
294 of a single layer of basic filtration media. In this part of the study, this assumption and equation
295 are examined in the context of the tested composite filter samples.

296 Figure 6 shows the comparison between the collection efficiency calculated by Eq. (3) and
297 the measured collection efficiency for the composite filter samples made of multiple layers of basic
298 media C and F. The discrepancy between the measured and calculated collection efficiencies was
299 found for the composite samples in the test particle size range. For our test composite filter samples,
300 the measured efficiencies were less than the calculated ones in the test particle size range. Three
301 possible reasons for the above observed discrepancy: (1) the micro-structure uniformity of basic
302 filtration media, leading to an issue of any given layer not necessarily being representative of the
303 others in the calculation for overall collection efficiency; and (2) the loose layering of multiple
304 basic filtration media, resulting in a different interfacial microstructure between any two adjacent

305 layers (compared to that of basic media layers); (3) the change of charge status of test particles,
306 resulting in different collection efficiencies for different basic media layers. A supplementary
307 experiment was thus performed to test the potential explanations.

308 The composite filter sample with three layers of basic furnace media F was selected for
309 this supplementary experiment. The particle penetration of three basic filter media and the
310 composite filter were individually measured under the same face velocity of 10.5 cm/sec and using
311 DMA-classified particles of 50, 100 and 200 nm in sizes. The product of the measured penetration
312 data of the three basic furnace filter media (i.e., $P=P_1*P_2*P_3$, where P_i is the particle penetration
313 of the basic media, i) was compared to the measured penetration of the composite sample. Three
314 composite filter samples were tested to calculate the average particle penetration efficiency for a
315 specific size. Figure 7 shows the comparison between the calculated and measured collection
316 efficiencies obtained in this experiment. It was found that the measured particle collection
317 efficiencies of the three-layered composite filter samples were again lower than the calculated,
318 especially when using small particle sizes. The result above is consistent with the trend observed
319 in Figure 6. It was thus concluded that the discrepancy shown in Fig. 6 was not primarily due to
320 the uniformity of the media microstructure. The observed discrepancy in the particle collection
321 should be attributed to either the loose assembly of the multiple layers of basic filtration media or
322 the charge status change of challenging particles. Further investigation will be required to identify
323 the reason(s).

324 **4. Conclusions**

325 The size-dependent collection efficiency of four face masks and one N95 FFR were
326 measured under the same testing protocol. Test filter media samples were challenged with
327 neutralized DMA-classified NaCl particles between the sizes of 20-800 nm and at a face velocity

328 of 10.5 cm/s. Two CPCs were used to measure the number concentration of particles upstream and
329 downstream of the filter holder in which a test filter sample resided. The particle penetration of a
330 test filter sample was calculated by taking the ratio of the downstream to the upstream particle
331 concentrations. The pressure drop across the filter sample was also measured for the FOM (Figure
332 of Merit) calculation. As expected, the minimum particle collection efficiency of the N95 FFR
333 sample was higher than 95% and the minimum collection efficiency of all the face mask samples
334 varied from 71.8% to 83.6%. The MPPS for the N95 FFR and face masks were all ~50 nm in this
335 study. The N95 respirator had a higher FOM value than the face masks.

336 The strategy of using multiple layers of basic filtration media to construct a composite filter
337 with a particle collection efficiency comparable to that of N95 FFRs (as an alternative media for
338 N95 respirators) has been investigated. The basic filtration media selected in this study were face
339 mask media and MERV13 furnace filter media (because they are readily available on the market).
340 Our data shows that composite filters made of double/triple layers of face mask media can provide
341 a comparable collection efficiency to a N95 FFR, especially for particles larger than 100 nm.
342 Although the collection efficiency of the composite filter with three layers of furnace filter media
343 was less than that of the N95 respirator sample for particles less than 100 nm in size, the three-
344 layered composite filter was able to provide a comparable collection efficiency for particles larger
345 than 100 nm in diameter. The composite filter with five layers of furnace filter media could provide
346 a collection efficiency like that of N95 respirator media in the test particle size range. Moreover,
347 the composite samples of multi-layered face mask media had the lowest FOM, while the sample
348 of multi-layered furnace media offered the highest FOM. The use of composite filters composed
349 of multiple layers of basic furnace filter media is therefore the preferred option as an alternative
350 media for a N95 respirator, given the current N95 respirator shortage.

351 The additivity of the particle collection efficiency for composite filters assembled from
352 multiple layers was also examined. The discrepancy between the measured and calculated
353 collection efficiencies of multi-layered composite samples (when loosely layered) was found. An
354 additional experiment showed that the observed discrepancy was either due to the possible
355 differences in the interfacial microstructure in a composite filter or the charge status change of the
356 challenging particles during the particle collection, not the uniformity of basic filter media.

ACCEPTED MANUSCRIPT

357 **Acknowledgements**

358 The authors thank the partial financial support of the members in the Center for Filtration Research,
359 University of Minnesota: 3M Corporation, A.O. Smith Company, Applied Materials, Inc., BASF
360 Corporation, Boeing Company, Corning Co., China Yancheng Environmental Protection Science
361 and Technology City, Cummins Filtration Inc., Donaldson Company, Inc., Entegris, Inc., Ford
362 Motor Company, Guangxi Wat Yuan Filtration System Co., Ltd, MSP Corporation; Samsung
363 Electronics Co., Ltd., Xinxiang Shengda Filtration Technology Co.,Ltd., TSI Inc., W. L. Gore &
364 Associates, Inc., Shigematsu Works Co., Ltd., and the affiliate member National Institute for
365 Occupational Safety and Health (NIOSH). Dr. Liu also thank the financial support by the China
366 Scholarship Council (No. 201906445004).

367 **References**

- 368 Balazy, A., Toivola, M., Adhikari, A., Sivasubramani, S.K., Reponen, T. and Grinshpun, S.A.
369 (2006a). Do N95 Respirators Provide 95% Protection Level against Airborne Viruses, and
370 How Adequate Are Surgical Masks? *Am. J. Infect. Control* 34: 51-57.
- 371 Balazy, A., Toivola, M., Reponen, T., Podgorski, A., Zimmer, A. and Grinshpun, S.A. (2006b).
372 Manikin-Based Performance Evaluation of N95 Filtering-Facepiece Respirators
373 Challenged with Nanoparticles. *Ann. Occup. Hyg.* 50: 259-269.
- 374 Brosseau, L.M., McCullough, N.V. and Vesley, D. (1997). Mycobacterial Aerosol Collection
375 Efficiency of Respirator and Surgical Mask Filters under Varying Conditions of Flow and
376 Humidity. *Appl. Occup. Environ. Hyg.* 12: 435-445.
- 377 Cho, K.J., Jones, S., Jones, G., McKay, R., Grinshpun, S.A., Dwivedi, A., Shukla, R., Singh, U.
378 and Reponen, T. (2010). Effect of Particle Size on Respiratory Protection Provided by Two
379 Types of N95 Respirators Used in Agricultural Settings. *J. Occup. Environ. Hyg.* 7: 622-
380 627.
- 381 Cowling, B., Zhou, Y., Ip, D., Leung, G. and Aiello, A. (2010). Face Masks to Prevent
382 Transmission of Influenza Virus: A Systematic Review. *Epidemiol. Infect.* 138: 449-456.
- 383 Davidson, C.S., Green, C.F., Gibbs, S.G., Schmid, K.K., Panlilio, A.L., Jensen, P.A. and Scarpino,
384 P.V. (2013). Performance Evaluation of Selected N95 Respirators and Surgical Masks
385 When Challenged with Aerosolized Endospores and Inert Particles. *J. Occup. Environ.*
386 *Hyg.* 10: 461-467.
- 387 Eninger, R.M., Honda, T., Adhikari, A., Heinonen-Tanski, H., Reponen, T. and Grinshpun, S.A.
388 (2008). Filter Performance of N99 and N95 Facepiece Respirators against Viruses and
389 Ultrafine Particles. *Ann. Occup. Hyg.* 52: 385-396.

390 Eshbaugh, J.P., Gardner, P.D., Richardson, A.W. and Hofacre, K.C. (2009). N95 and P100
391 Respirator Filter Efficiency under High Constant and Cyclic Flow. *J. Occup. Environ. Hyg.*
392 6: 52-61.

393 Gralton, J., Tovey, E., McLaws, M.L. and Rawlinson, W.D. (2011). The Role of Particle Size in
394 Aerosolised Pathogen Transmission: A Review. *J. Infect.* 62: 1-13.

395 He, X., Reponen, T., McKay, R.T. and Grinshpun, S.A. (2013). Effect of Particle Size on the
396 Performance of an N95 Filtering Facepiece Respirator and a Surgical Mask at Various
397 Breathing Conditions. *Aerosol Sci. Technol.* 47: 1180-1187.

398 Huang, S.-H., Chen, C.-W., Kuo, Y.-M., Lai, C.-Y., McKay, R. and Chen, C.-C. (2013). Factors
399 Affecting Filter Penetration and Quality Factor of Particulate Respirators. *Aerosol Air Qual.*
400 *Res.* 13: 162-171.

401 Kutter, J.S., Spronken, M.I., Fraaij, P.L., Fouchier, R.A. and Herfst, S. (2018). Transmission
402 Routes of Respiratory Viruses among Humans. *Curr. Opin. Virol.* 28: 142-151.

403 Lee, S.A., Grinshpun, S.A. and Reponen, T. (2008). Respiratory Performance Offered by N95
404 Respirators and Surgical Masks: Human Subject Evaluation with NaCl Aerosol
405 Representing Bacterial and Viral Particle Size Range. *Ann. Occup. Hyg.* 52: 177-185.

406 Liu, Y., Gayle, A.A., Wilder-Smith, A. and Rocklöv, J. (2020). The Reproductive Number of
407 Covid-19 Is Higher Compared to Sars Coronavirus. *J. Travel Med.*

408 MacIntyre, C.R., Cauchemez, S., Dwyer, D.E., Seale, H., Cheung, P., Browne, G., Fasher, M.,
409 Wood, J., Gao, Z. and Booy, R. (2009). Face Mask Use and Control of Respiratory Virus
410 Transmission in Households. *Emerg. Infect. Dis.* 15: 233.

411 Oberg, T. and Brosseau, L.M. (2008). Surgical Mask Filter and Fit Performance. *Am. J. Infect.*
412 *Control* 36: 276-282.

413 Prompetchara, E., Ketloy, C. and Palaga, T. (2020). Immune Responses in Covid-19 and Potential
414 Vaccines: Lessons Learned from Sars and Mers Epidemic. *Asian Pac. J. Allergy Immunol.*
415 38: 1-9.

416 Rengasamy, S., Eimer, B.C. and Shaffer, R.E. (2009). Comparison of Nanoparticle Filtration
417 Performance of Niosh-Approved and Ce-Marked Particulate Filtering Facepiece
418 Respirators. *Ann. Occup. Hyg.* 53: 117-128.

419 Rengasamy, S., King, W.P., Eimer, B.C. and Shaffer, R.E. (2008). Filtration Performance of
420 Niosh-Approved N95 and P100 Filtering Facepiece Respirators against 4 to 30 Nanometer-
421 Size Nanoparticles. *J. Occup. Environ. Hyg.* 5: 556-564.

422 Rengasamy, S., Miller, A. and Eimer, B.C. (2011). Evaluation of the Filtration Performance of
423 Niosh-Approved N95 Filtering Facepiece Respirators by Photometric and Number-Based
424 Test Methods. *J. Occup. Environ. Hyg.* 8: 23-30.

425 Romay, F.J., Liu, B.Y. and Chae, S.-J. (1998). Experimental Study of Electrostatic Capture
426 Mechanisms in Commercial Electret Filters. *Aerosol Sci. Technol.* 28: 224-234.

427 Stelzer - Braid, S., Oliver, B.G., Blazey, A.J., Argent, E., Newsome, T.P., Rawlinson, W.D. and
428 Tovey, E.R. (2009). Exhalation of Respiratory Viruses by Breathing, Coughing, and
429 Talking. *J. Med. Virol.* 81: 1674-1679.

430 Wilder-Smith, A., Chiew, C.J. and Lee, V.J. (2020). Can We Contain the Covid-19 Outbreak with
431 the Same Measures as for Sars? *Lancet Infect. Dis.*

432 Willeke, K., Qian, Y., Donnelly, J., Grinshpun, S. and Ulevicius, V. (1996). Penetration of
433 Airborne Microorganisms through a Surgical Mask and a Dust/Mist Respirator. *Am. Ind.*
434 *Hyg. Assoc. J.* 57: 348-355.

435 World Health Organization (2014). Infection Prevention and Control of Epidemic-and Pandemic-
436 Prone Acute Respiratory Infections in Health Care, World Health Organization.

437 Xie, X., Li, Y., Chwang, A., Ho, P. and Seto, W. (2007). How Far Droplets Can Move in Indoor
438 Environments--Revisiting the Wells Evaporation-Falling Curve. *Indoor Air* 17: 211-225.

439 Yang, S., Lee, G.W., Chen, C.-M., Wu, C.-C. and Yu, K.-P. (2007). The Size and Concentration
440 of Droplets Generated by Coughing in Human Subjects. *J. Aerosol Med.* 20: 484-494.

441 Zhu, N., Zhang, D., Wang, W., Li, X., Yang, B., Song, J., Zhao, X., Huang, B., Shi, W. and Lu, R.
442 (2020). A Novel Coronavirus from Patients with Pneumonia in China, 2019. *New Engl. J.*
443 *Med.*

444 Zuo, Z., Kuehn, T.H. and Pui, D.Y. (2013). Performance Evaluation of Filtering Facepiece
445 Respirators Using Virus Aerosols. *Am. J. Infect. Control* 41: 80-82.

446

447

List of Tables

448 Table 1 The label designation of studied filter media samples from four face masks and
449 one N95 FFR media and their rated particle filtration efficiency (given by the
450 manufacturer).

451 Table 2 Summary of the measured pressure drop of all the test filter samples (with basic
452 media and composite media) at the face velocity of 10.5 cm/s

ACCEPTED MANUSCRIPT

List of Figures

- Figure 1 Schematic diagram of the experimental setup used in this study
- Figure 2 The measured size-fractionated efficiency of the FFR and face mask samples at the face velocity of 10.5 cm/s
- Figure 3 The size-fractionated figure of merit (FOM) of the FFR and face mask samples at the face velocity of 10.5 cm/s
- Figure 4 The size-fractionated collection efficiency of the composite filter samples composed of multiple layers of basic face mask and furnace media (loosely layered) at the face velocity of 10.5 cm/s
- Figure 5. The comparison on the FOM of the N95 FFR and composite filter samples at the face velocity of 10.5 cm/s
- Figure 6. Comparison of the measured and calculated collection efficiency of composite filter samples with multiple layers of basic media C and F at the face velocity of 10.5 cm/s. Note that this calculation was based on the particle collection efficiency of a basic media (randomly selected).
- Figure 7. Comparison of the measured and calculated collection efficiency of composite filter samples having triple layers of basic media F at the particle sizes of 50, 100 and 200 nm (measured at the face velocity of 10.5 cm/s). Note that this calculation was based on the measured particle collection efficiency of individual basic media layers used to construct the composite filters.

Table 1

Sample Label	Type of Masks	Rated Filtration efficiency (by the manufacturers)
A	N95 particulate FFRs	$\geq 95\%$, NIOSH certified
B	Tie-on face surgical mask,	NA
C	Ear-loop procedure mask	ASTM Level 1 (BFE $\geq 95\%$, PFE $\geq 95\%$)
D	Ear-loop face mask (with cocoanut shell activated carbon)	$\geq 98\%$ for particles larger than 3.1 μm
E	Ear-loop medical mask	BFE $\geq 95\%$
F	Furnace filter media	MERV 13

ACCEPTED MANUSCRIPT

Table 2

Media Sample	Pressure drop (Pa)	Composite Samples	Pressure drop (Pa)
A	81.1±4.9	B_double layers	95.2±8.4
B	45.1±7.7	B_triple layers	158.0±15.4
C	64.3±5.1	C_double layers	127.7±11.9
D	67.7±6.2	D_double layers	120.2±10.2
E	59.6±4.6	E_double layers	128.7±3.9
F	9.3±1.2	F_triple layers	30.0±2.0
		F_five layers	50.6±0.7

ACCEPTED MANUSCRIPT

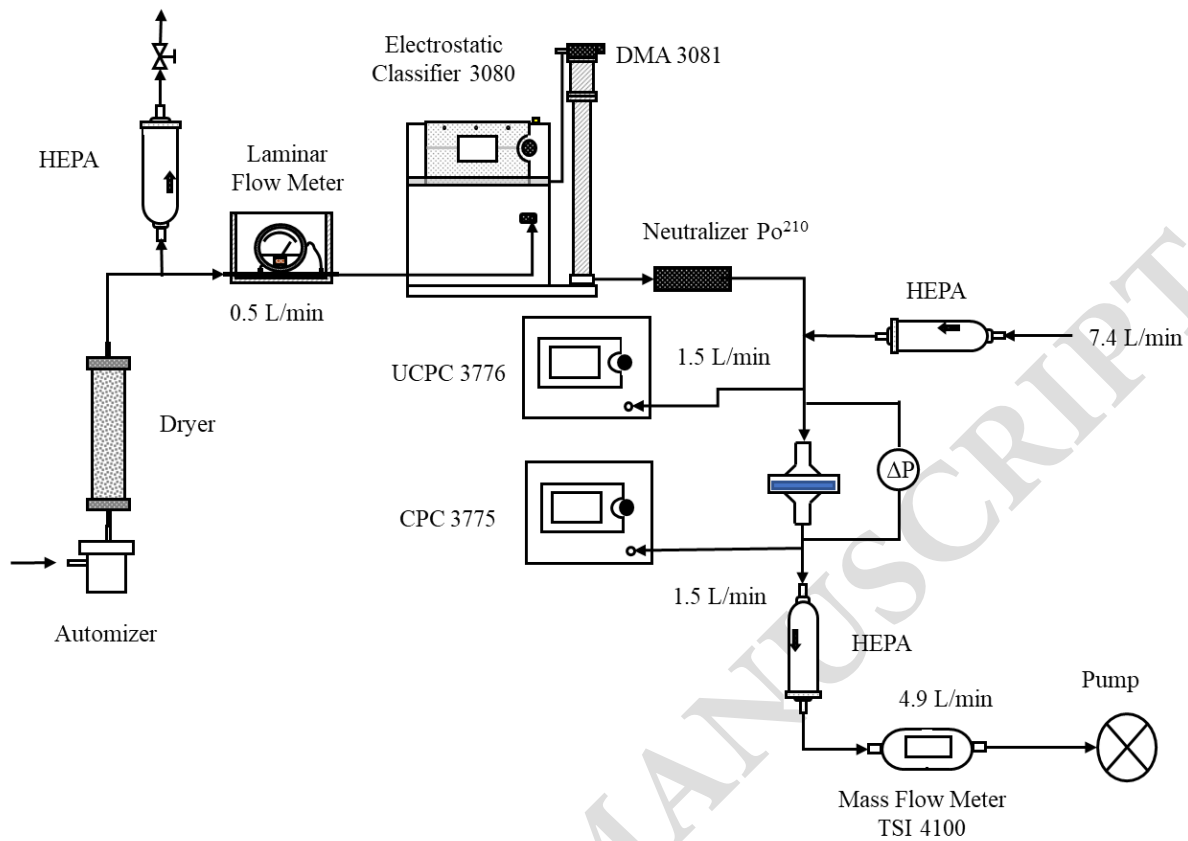


Figure. 1

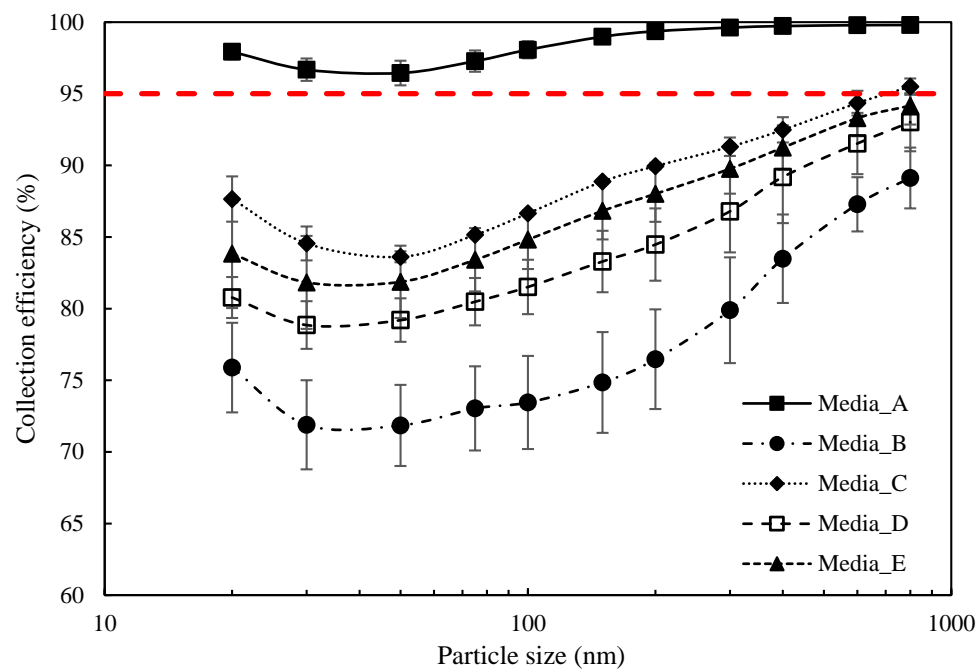


Figure. 2

ACCEPTED MANUSCRIPT

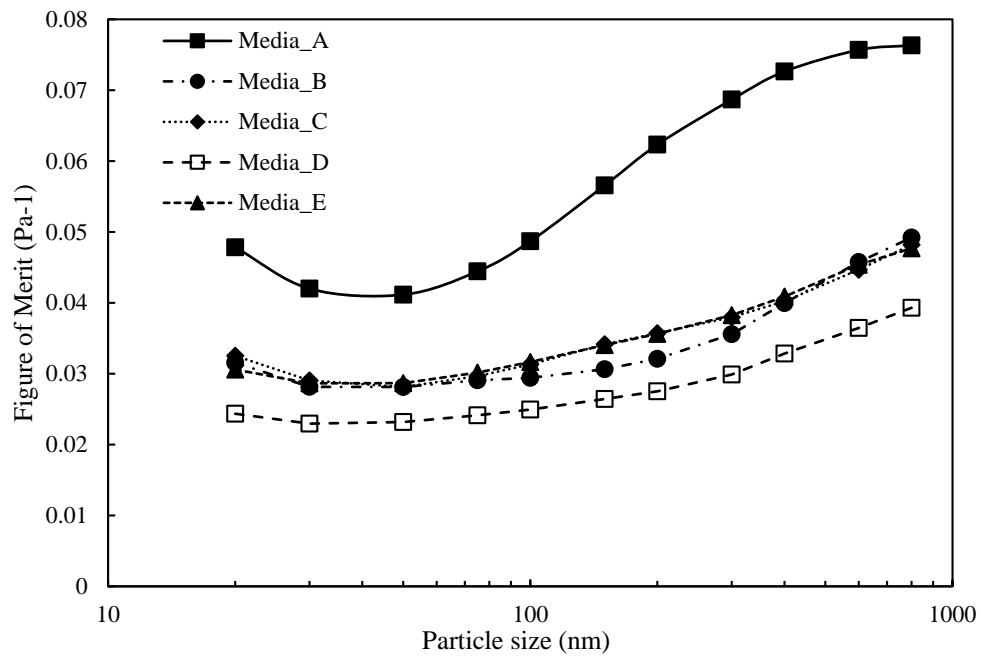


Figure. 3

ACCEPTED MANUSCRIPT

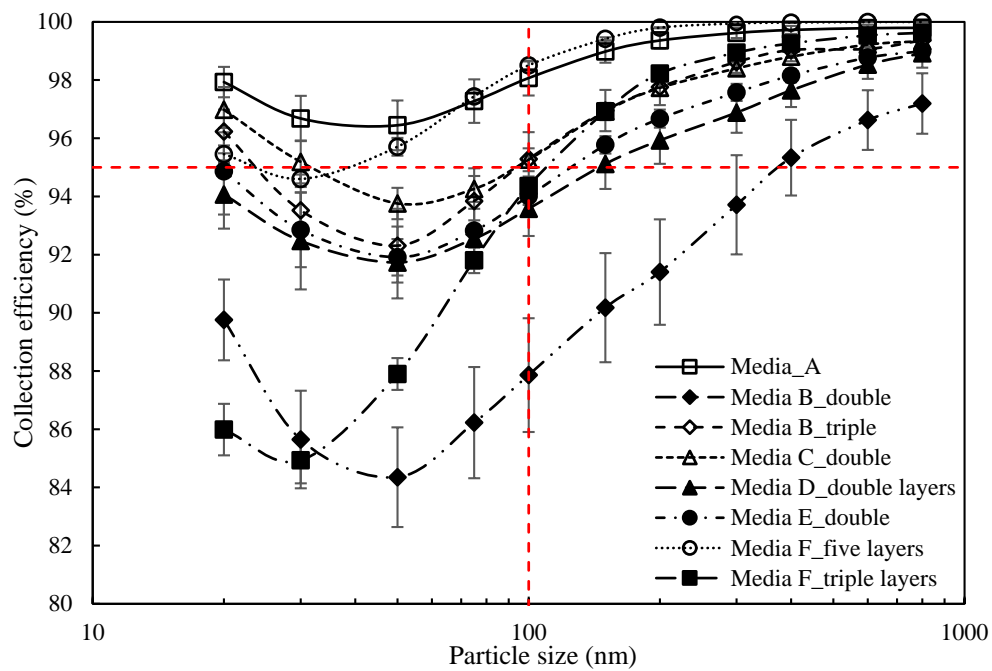


Figure. 4

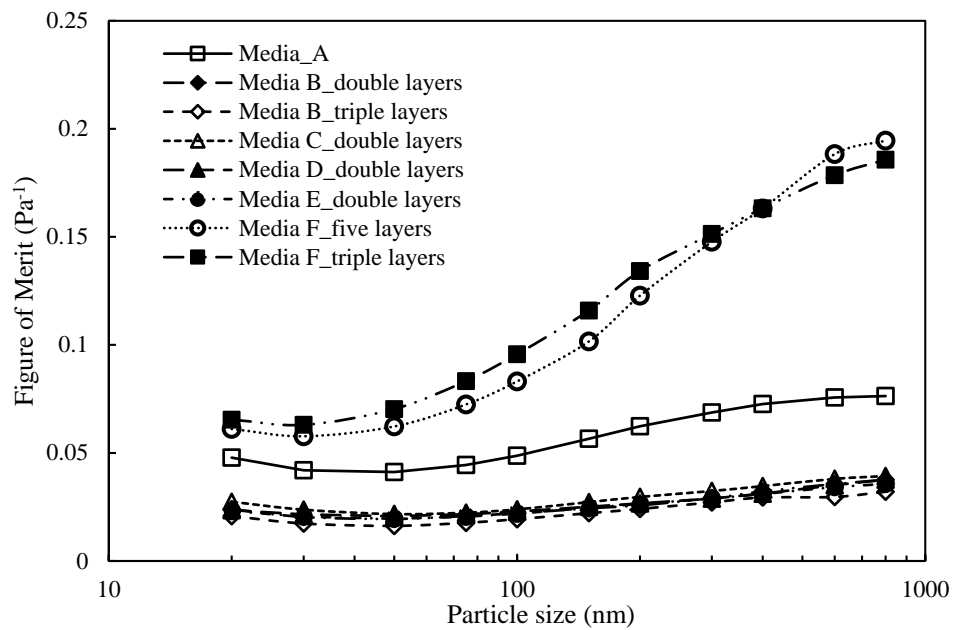


Figure. 5

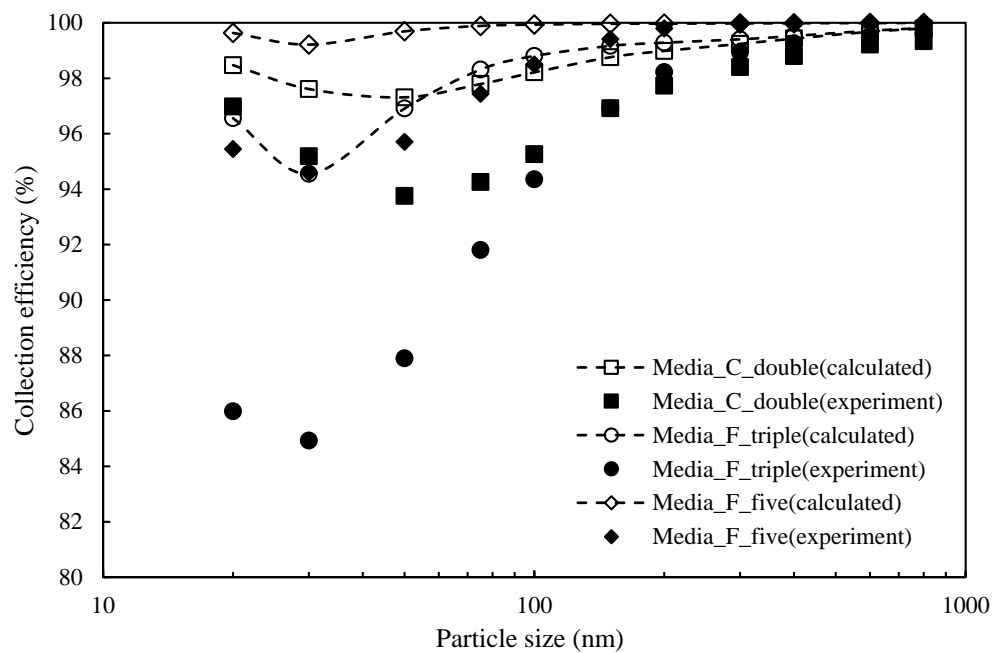


Figure. 6

ACCEPTED MANUSCRIPT

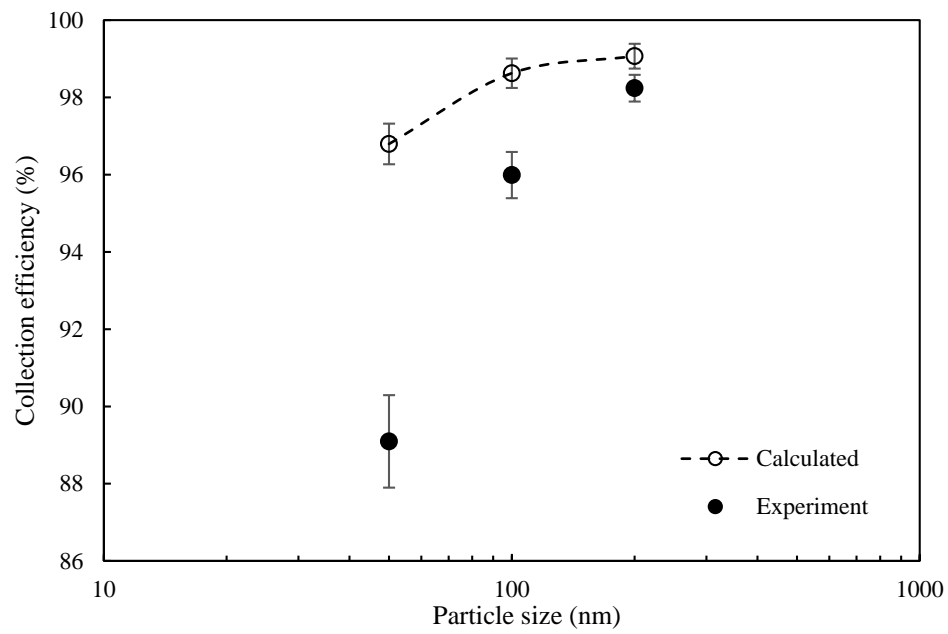


Figure 7

ACCEPTED MANUSCRIPT